HHS Public Access

Author manuscript

Cancer Res. Author manuscript; available in PMC 2020 February 15.

Published in final edited form as:

Cancer Res. 2019 August 15; 79(16): 4113–4123. doi:10.1158/0008-5472.CAN-18-4093.

Inactivation of *Bap1* Cooperates with Losses of *Nf2* and *Cdkn2a* to Drive the Development of Pleural Malignant Mesothelioma in Conditional Mouse Models

Anna-Mariya Kukuyan[1], **Eleonora Sementino**[1], **Yuwaraj Kadariya**[1], **Craig W. Menges**[1], **Mitchell Cheung**[1], **Yinfei Tan**[1], **Kathy Q. Cai**[2], **Michael J. Slifker**[3], **Suraj Peri**[3], **Andres J. Klein-Szanto**[2], **Frank J. Rauscher III**[4], **Joseph R. Testa**[1]

[1]Cancer Biology Program, Fox Chase Cancer Center, Philadelphia, PA, USA

[2]Histopathology Facility, Fox Chase Cancer Center, Philadelphia, PA, USA

[3]Bioinformatics and Biostatistics Facility, Fox Chase Cancer Center, Philadelphia, PA, USA

[4]Wistar Institute, Philadelphia, PA, USA

Abstract

Pleural malignant mesothelioma (MM) is a therapy-resistant cancer affecting the serosal lining of the thoracic cavity. Mutations/deletions of *BAP1*, *CDKN2A*, and *NF2* are the most frequent genetic lesions in human MM. We introduced various combinations of these deletions in the pleura of conditional knockout (CKO) mice, focusing on the contribution of *Bap1* loss. While homozygous CKO of *Bap1*, *Cdkn2a*, or *Nf2* alone gave rise to few or no MMs, inactivation of *Bap1* cooperated with loss of either *Nf2* or *Cdkn2a* to drive development of MM in ~20% of double-CKO mice, and a high incidence (22/26, 85%) of MMs was observed in *Bap1;Nf2;Cdkn2a* (triple)-CKO mice. MM onset was rapid in triple-CKO mice, with a median survival of only 12 weeks, and MMs from these mice were consistently high-grade and invasive. Adenoviral-Cre treatment of normal mesothelial cells from *Bap1;Nf2;Cdkn2a* CKO mice, but not from mice with knockout of one or any two of these genes, resulted in robust spheroid formation *in vitro,* suggesting that mesothelial cells from *Bap1;Nf2;Cdkn2a* mice have stem cell-like potential. RNA-seq analysis of MMs from triple-CKO mice revealed enrichment of genes transcriptionally regulated by the polycomb repressive complex 2 (PRC2) and others previously implicated in known Bap1-related cellular processes. These data demonstrate that somatic inactivation of *Bap1*, *Nf2,* and *Cdkn2a* results in rapid, aggressive MMs, and that deletion of *Bap1* contributes to tumor development, in part, by loss of PRC2-mediated gene repression of tumorigenic target genes and by acquisition of stem-cell potential, suggesting a potential avenue for therapeutic intervention.

Correspondence: Joseph R. Testa, Ph.D., Fox Chase Cancer Center, 333 Cottman Avenue, Philadelphia, PA 1911; Phone: (215) 728-2610; Fax: (215) 214-1619; joseph.testa@fccc.edu.

Conflict of Interest Statement

JRT and MC have a pending patent application on *BAP1* mutation testing. JRT has provided legal consultation regarding genetic aspects of mesothelioma. The remaining authors have no potential conflicts of interest with regard to the publication of this work.

Keywords

Mesothelioma; tumor suppressors genes; conditional knockout mice; hepatic carcinomas; polycomb repressor complex 2

Introduction

Pleural malignant mesothelioma (MM) is an aggressive, treatment-resistant cancer, which is causally related to asbestos exposure. Early cytogenetic and deletion mapping studies had uncovered several prominent sites of chromosomal loss in human pleural MM, including 3p21, 9p21 and 22q12, and these recurrent abnormalities often occurred in combination in a given tumor, suggesting a multi-step pathogenetic process (1). Alterations in the target tumor suppressor genes at two of these sites, i.e., *CDKN2A* at 9p21 and *NF2* at 22q12, were first discovered more than two decades ago (2–6), whereas the identity of the crucial 3p21 gene in MM remained a mystery until 2011, when *BAP1* was identified as the critical MM tumor suppressor gene at this location (7,8). In a recent comprehensive study as part of The Cancer Genome Atlas, somatic genetic alterations of *BAP1*, *NF2* and *CDKN2A* were observed in combination in 25/74 (34%) pleural MMs (9).

The alterations of *CDKN2A* involve heterozygous or homozygous deletions of all or part of the locus (2). Abnormalities of *NF2* in MM frequently are biallelic, consisting of both an inactivating mutation and loss of the second allele (10). Biallelic losses of *CDKN2A* have been documented in ~40% of primary MMs (7) and up to 90% of MM cell lines (2), whereas inactivating *NF2* mutations have been reported in 20-55% of cases (5–7,10). Using Sanger sequencing, somatic inactivating mutations of *BAP1* were initially reported in 20-25% of sporadic MMs (7,8), but more recent studies with other sequencing platforms such as targeted next generation sequencing and multiplex ligation-dependent probe amplification have uncovered *BAP1* alterations in ~60% of cases, with a preponderance of exonic deletions (11).

The *CDKN2A* locus encodes the tumor suppressors p16INK4A and p14ARF, which regulate the Rb and p53 cell cycle pathways, respectively. In MM, the deleted region of *CDKN2A* typically includes exon 2 (2), which encodes portions of p16INK and p14ARF, and is thus predicted to affect both Rb and p53 pathways. Re-expression of p16INK4A in MM cells results in cell cycle arrest and tumor suppression/regression (12), while re-expression of p14ARF in MM cells induces G1 arrest/apoptosis (13). Underscoring the relevance of *Cdkn2a* to MM pathogenesis, heterozygous *Cdkn2a* knockout mice treated with asbestos develop MM at a significantly accelerated rate compared to asbestos-treated wild-type (WT) littermates (14). Additionally, mice deficient for both p16Ink4a and p19Arf exhibit enhanced asbestos-induced MM formation relative to mice deficient for either 16Ink4a or 19Arf alone (14).

Loss of the *NF2* product, Merlin, in MM leads to cell cycle progression by upregulation of cyclin D1 both transcriptionally (15) and post-transcriptionally via activation of mTORC1 (16). NF2 also inhibits Pak and FAK signaling, which play key roles in cell migration and spreading, respectively, and inactivation of *NF2* in MM cells promotes invasiveness and

spreading (17,18). *Nf2*$^{+/-}$ mice treated with asbestos develop MM at an accelerated rate compared to asbestos-treated WT mice, suggesting that merlin inactivation contributes significantly to MM development (4,19,20). Moreover, mice with heterozygous losses of both *Nf2* and *Cdkn2a* show further acceleration of asbestos-induced MM, with resulting tumors exhibiting increased cancer stem cells and enhanced tumor spreading capability compared to that observed in mice with losses of only one or the other of these genes (21). Similarly, conditional knockout (CKO) mice harboring homozygous deletions of both *Nf2* and *p16Ink4a/19Arf* in the mesothelial lining of the thoracic cavity developed a high incidence of pleural MM that showed increased pleural invasion compared to *Nf2;Tp53* CKO mice (20).

BRCA1-associated protein-1 (BAP1) was discovered as an ubiquitin hydrolase that associates with the RING finger domain of BRCA1 and enhances BRCA1-mediated inhibition of breast cancer cell growth (22). BAP1 interacts with ASXL family members to form the polycomb group (PcG) repressive deubiquitinase (PR-DUB) complex involved in stem cell pluripotency and other developmental processes (23). BAP1 also interacts with and deubiquitinates the transcriptional regulator host cell factor 1 (HCF1) (24). Importantly, BAP1 has been shown to form complexes with numerous transcription factors and cofactors, including transcription factor YY1 (25). The BAP1 ubiquitin carboxyl hydrolase activates transcription in an enzyme-dependent manner and regulates the expression of a variety of genes involved in numerous processes, including cell proliferation, DNA damage and inflammatory responses, metabolism, and various mechanisms of cell death (24,26–29). In animal models, asbestos exposure induces a significant increase in the incidence of MM in heterozygous *Bap1*-mutant mice as compared to asbestos-exposed WT littermates (30,31).

MM patients with germline *BAP1* mutations have an improved long-term survival compared to MM patients without such heritable variants (32,33). However, it remains unclear whether somatic *BAP1* mutations/deletions are associated with a poor prognosis in sporadic MM, as is the case in uveal melanoma and renal cell carcinoma (34,35). While most human MMs exhibit somatic alterations of *BAP1*, *NF2* and/or *CDKN2A*, currently it is not known if inactivation of *BAP1* cooperates with loss of *NF2* and/or *CDKN2A* to drive a more aggressive MM phenotype. Here we address these questions experimentally using CKO models.

Materials and Methods

Mouse strains and genotyping

All mouse studies were performed in accordance with a protocol approved by the Fox Chase Cancer Center (FCCC) IACUC. *Nf2*$^{f/f}$;*Cdkna*$^{f/f}$ mice in FVB/N genetic background (20), a gift of Anton Berns, were maintained in our laboratory in a mixed FVB/N × 129/Sv background. The LoxP sites in the *Cdkn2a* locus of these mice permit excision of exon 2, which results in inactivation of both p16Ink4a and p19Arf.

Bap1$^{f/f}$ mice in FVB/N background were developed in our laboratory using zinc finger nuclease (ZFN) technology, with the assistance of the FCCC Transgenic Mouse Facility. Custom ZFNs targeting *Bap1* were designed and validated in mammalian cells by Sigma-

Aldrich (St. Louis, MO). A pair of ZFNs was identified that binds to and cuts within a site in intron 5 of *Bap1* with high efficiency and specificity. We then designed a donor DNA construct containing LoxP sites in introns 6 and 7 (Figure 1A), such that upon adenovirus-mediated expression of Cre recombinase there is deletion of exon 7 of *Bap1*. The ZFN mRNAs and donor DNA were injected into the pronucleus of one-cell embryos of FVB/N mice, and embryos were then transferred into pseudo-pregnant females. DNA from pups was analyzed for correct targeting by PCR amplification of the gene and sequencing. Three founder mice with LoxP sites integrated in the *Bap1* locus were identified, one of which was used for experiments reported here. Representative examples of genotyping of DNA from *Bap1* CKO mice are shown in Figure 1B.

In addition to $Bap1^{f/f}$, $Nf2^{f/f}$, and $Cdkn2a^{f/f}$ mice, these CKO animals were crossed to generate cohorts with the following genotypes: $Bap1^{f/f}$;$Nf2^{f/f}$, $Bap1^{f/f}$;$Cdkn2a^{f/f}$, $Nf2^{f/f}$;$Cdkn2a^{f/f}$ and $Bap1^{f/f}$;$Nf2^{f/f}$;$Cdkn2a^{f/f}$. The following primers and annealing temperatures were used for genotyping: $Bap1^{f/f}$ 1063: 5'-CCC TGA GAC CCA GAA AAT CA-3', Tm = 54.3°C; $Bap1^{f/f}$ 1228: 5'-GGG AGG CTC TTT GAA TTG GA-3', Tm = 54.9°C; $Nf2^{f/f}$ 1048: 5'-CTT CCC AGA CAA GCA GGG TTC-3', Tm = 58.0°C; $Nf2^{f/f}$ 1049: 5'-GAA GGC AGC TTC TTC CTT AAG TC-3', Tm = 53.2°C; $Cdkn2a^{f/f}$ 1025: 5'-GCA GTG TTG CAG TTT GAA CCC-3', Tm = 57.4°C; and $Cdkn2a^{f/f}$ 1026: 5'-TGT GGC AAC TGA TTC AGT TGG-3', Tm = 55.8°C.

Adeno-Cre injections

Ad5CMVCre (Adeno-Cre) virus was obtained from the Viral Vector Core of the University of Iowa. Mice 8-12-weeks of age were injected intrathoracically (20), specifically intrapleurally, with Adeno-Cre virus (50 μl of 3-6 × 10^{10} PFU), with approximately equal numbers of mice of each gender in each cohort. Mice were monitored daily and were euthanized upon visible signs of distress, including extreme fatigue, labored breathing, or when mice exhibited a 10% change in body weight. Tissues of all organs of the pleural and peritoneal cavities were collected from sacrificed mice, and tumor specimens were subjected to histopathological assessment. Portions of tumors were also saved in both O.C.T. Compound and RNA*later* Solution (Thermo Fisher, Waltham, MA) and immediately frozen at −80°C.

Tumor histopathology, immunohistochemistry and RT-PCR analysis

The histopathological procedures used are essentially the same as previously described (23). In summary, after paraffin embedding, sectioning and deparaffinization, hematoxylin and eosin (H&E)-stained sections were used for histopathologic evaluation, and unstained sections were used for immunohistochemistry (IHC). For IHC, sections were subjected to heat-induced epitope retrieval using citrate buffer (pH 6.0) for 20 min.

MMs were diagnosed by two independent pathologists (A.J.K.-S. and K.Q.C.). To confirm the diagnosis of MM, IHC was performed for various MM markers, including mesothelin, detected with D-16 antibody (Santa Cruz Biotechnology, Dallas, TX), and cytokeratin 8, detected with TROMA-1 antibody (DSHB, University of Iowa, Iowa City, IA). In addition, reverse transcription-PCR (RT-PCR) analysis was also performed to analyze MM markers,

including *Wt1*, *Msln* (mesothelin), and *Krt18/19* (cytokeratin 18/19). RT-PCR analysis for *Msln* used primers 5′-ATCAAGACATTCCTGGGTGGG-3′ and 5′-CGGTTAAAGCTGGGAGCAGAG-3′. Primers for other MM markers have been previously described (4). To assess cell proliferation, IHC staining was performed with antibodies for Ki-67 (Dako/Agilent, Santa Clara, CA).

Immunoblot analysis and antibodies

Immunoblots were prepared with 30-50 μg of protein lysate per sample, as previously described (21). Anti-Bap1 antibody (A302-243, 1:2000) was purchased from Bethyl Laboratories (Montgomery, TX). Anti-Bap1 (C-4, sc-28383, 1:2000), anti-p19Arf (5-C3-1, sc-32748 1:1000), anti-Gapdh (6C5, sc-32233, 1:50,000), and anti-β-actin (C4, sc-47778, 1:50,000) were from Santa Cruz Biotechnology; anti-Nf2 (D1D8, #6995S, 1:1000), anti-total-Akt (#9272S, 1:1000), and anti-P-Akt, Ser473 (D9E XP, #4060, 1:1000) were from Cell Signaling Technology (Danvers, MA); and anti-p16 (ab189034 1:1000) was from Abcam (Cambridge, MA). Immunoblots were imaged using Immobilon Western Chemiluminescent HRP Substrate (EMD Millipore, Ontario Canada; P90720 Cat. No. WBKLS0500).

Spheroid growth assay

Primary normal mesothelial cells were isolated from individual CKO mice, 10-12 weeks of age, with each of the following genotypes: $Bap1^{f/f}$, $Nf2^{f/f}$, $Cdkn2a^{f/f}$, $Bap1^{f/f};Nf2^{f/f}$, $Bap1^{f/f};Cdkn2a^{f/f}$, $Nf2^{f/f};Cdkn2a^{f/f}$, and $Bap1^{f/f};Nf2^{f/f};Cdkn2a^{f/f}$. The mesothelial cells were isolated by sacrificing animals and adding trypsin (0.25% Trypsin-EDTA, Gibco, 25200-056) to the peritoneal cavity, according to the method of Bot et al. (36). Normal mesothelial cells at passage 2 were then seeded in 6-well plates (Thermo Fisher BioLite 6-well Multidish, Cat. #130184) and treated with 4×10^{10} PFU/ml of either control Ad5CMVempty (Adeno-CMV) or Adeno-Cre virus for 1 h. Cells were then washed in PBS, cultured in normal mesothelial media (34) for 72 h, and trypsinized. Next, 5,000 mesothelial cells were seeded in each well of a 6-well non-adherent plate (Corning, Costar) in serum-free DMEM/F12 media supplemented with B27, EGF (10 ng/mL), basic FGF (10 ng/mL) and penicillin/streptomycin, as described (21). The experiment was performed in triplicate for each cell genotype. Spheroids were photographed using light microscopy after 9 days of culture.

RNA-seq analysis

Tumor RNA was isolated in Trizol and purified with RNeasy columns (Qiagen, Germantown, MD). RNA-seq was performed with a HiSeq Sequencer and the following reagents: TruSeq Stranded mRNA Library, HiSeq Rapid SR Cluster, and HiSeq Rapid SBS v2 kits (Illumina, San Diego, CA). Stranded mRNA-seq libraries were prepared according to Illumina's product guide. First-strand cDNA was synthesized using SuperScript II reverse transcriptase (Thermo Fisher) and random primers at 42°C for 15 min, followed by second strand synthesis at 16°C for 1 h. Adapters with Illumina P5/P7 sequences and indices were ligated to cDNA fragments, and libraries were pooled and loaded onto the sequencer. Fastq files were aligned to the mm10 mouse genome using TopHat2. Raw sequence counts for each gene were produced with HTseq (https://htseq.readthedocs.io) and differentially

expressed genes were identified by DESeq2 (37). RNA-seq heatmaps were constructed from $\log_2(x+1)$-transformed counts/million, standardized across rows, using the "heatmap.2" function from the R *gplots* library. Raw sequencing data have been deposited in the GEO repository (accession number GSE131942).

Gene set enrichment analysis

For functional enrichment analysis, genes identified as differentially expressed by DESeq2 with nominal p-value < 0.5 were ranked by fold-change and mapped to human genes using R *biomaRt* (38). These genes were then analyzed using the GSEAPreranked method of Gene Set Enrichment Analysis (GSEA) (39) (with "classic" enrichment statistic) applied to the curated (c2) and Gene Ontology gene sets from the Molecular Signature Database (MSigDB). Confirmation of differentially expressed genes was performed by quantitative RT-PCR analysis; Taqman (Thermo Fisher) assay IDs used for 13 genes validated by RT-PCR analysis are shown in Supplemental Table 1.

Results

Temporal intrathoracic (IT) inactivation of *Bap1* together with *Nf2* and/or *Cdkn2a* results in MM and other tumors

Injection of Adeno-Cre virus into the pleural space of Rosa26 LacZ reporter (R26R) mice has been previously reported to result in efficient β-galactosidase expression in the mesothelial cell lining of the chest cavity (20). Locotemporal expression of Cre recombinase by IT injection of Adeno-Cre was used to induce mesothelial cell-specific loss of *Bap1*, *Nf2*, and/or *Cdkn2a* in homozygous single-gene CKO mice and in homozygous compound CKO mice. The injection scheme used for the CKO mice is depicted in Figure 1C. Tumors that arose in most mouse cohorts were mainly MMs, although other neoplasms were also observed (Table 1).

In the cohorts of mice with homozygous knockout of a single gene only, few MMs were seen. Among 32 $Bap1^{f/f}$ CKO mice injected IT with Adeno-Cre, a slow growing, well differentiated MM was identified in a single animal 45 weeks after injection. Interestingly, this MM acquired loss of Nf2 and p16Ink4a expression during tumor formation (Supplemental Figure 1A). As expected, this tumor showed Bap1 loss-related deficient deubiquitination activity; and consistent with the acquired loss of Nf2/Merlin, downstream Yap was not phosphorylated (Supplemental Fig. 1B). PCR analysis confirmed that losses of *Nf2* and *Cdkn2a* are acquired (Supplemental Figure 1C). MMs were observed in 2 of 15 $Nf2^{f/f}$ mice and 0 of 12 $Cdkn2a^{f/f}$ mice injected with Adeno-Cre, results comparable to those reported in an earlier study (20).

Among the IT-injected mice with homozygous inactivation of two genes, MMs were observed in 7 of 42 (16.6%) *Bap1;Nf2* CKO mice, 6 of 27 (22.2%) *Bap1;Cdkn2a* CKO mice, and 15 of 24 (62.5%) *Nf2;Cdkn2a* CKO mice. The highest incidence of MM (22 of 26, 84.6%) was observed in *Bap1*;*Nf2*;*Cdkn2a* triple-CKO mice. A summary of MM incidence among *Bap1* CKO mice and mice with the various compound CKO genotypes is shown in Figure 2A.

With regard to histological subtype, notably no epithelioid MMs were observed with any of the mouse genotypes. Sarcomatoid MMs predominated in most cohorts, with the exception being *Bap1*;*Nf2* CKO mice, in which 6 of 7 MMs showed mixed (biphasic) histology.

MM latency varied between 21 and 40 weeks among the different compound double-CKO mice. A markedly shorter MM latency, 12 weeks, was observed in *Bap1*;*Nf2*;*Cdkn2a* triple-CKO mice, a highly significant difference (log rank test, $p<0.0001$) from the 27 weeks observed for *Nf2*;*Cdkn2a* CKO mice or for any of the other compound double-CKO (DKO) mice. The MM survival differences between the three cohorts with different DKO combinations were not statistically significant (Supplemental Table 2). Kaplan-Meier survival curves of IT-injected mice that developed MM are shown in Figure 2B. Additionally, MMs from *Bap1*;*Nf2*;*Cdkn2a* CKO mice were consistently high-grade, very invasive, and highly proliferative tumors (Figure 3A,B), whereas MM morphology was generally more variable and less hypercellular with the other mouse genotypes. Immunoblotting confirmed the absence of expression of proteins encoded by conditionally knocked out genes *Bap1*, *Nf2* and *Cdkn2a* (p16Ink4a and p19Arf) in 12 of 12 MMs tested, and interestingly there was also acquired loss of expression of *Bap1* in 4 of 6 MMs from *Nf2;Cdkn2a* CKO mice (Figure 4). We also assessed the status of Akt in these tumors, because Akt activation occurs frequently in human and murine MMs (4). Akt activation was seen in all MMs tested, as indicated by expression of phosphorylated (active) Akt (Figure 4).

Besides MM, various other tumor types were also seen in mice injected IT with Adeno-Cre (Table 1). Among mice with homozygous inactivation of *Bap1* alone in the thoracic cavity, 2 lung adenocarcinomas and 1 lymphoma were seen. The remaining mice died of other age-related diseases, including bladder obstructions or lymphoproliferative diseases. Among the compound CKO mice, most notable was the cohort with inactivation of both *Bap1* and *Nf2*, which showed a high incidence (28 of 42, 66.7%) of hepatocellular carcinoma (HCC) and intrahepatic cholangiocarcinoma (ICC) (Supplemental Figure 2A and 2B, respectively), with these tumors generally arising later than MMs in this cohort (median 35 weeks vs. 21 weeks, respectively). Altogether, 28 *Bap1;Nf2* CKO mice developed hepatic cancers, including 7 with HCC alone, 4 with ICC alone, 14 with both HCC and ICC, 1 with HCC and MM, and 2 with HCC, ICC, and MM.

Inactivation of three MM driver tumor suppressor genes is sufficient to induce a stem cell-like phenotype in mesothelial cells

To assess the cooperativity of *Bap1*, *Nf2*, and *Cdkn2a* losses *in vitro*, we next used a spheroid growth assay. Primary normal mesothelial cells were isolated from $Bap1^{f/f}$, $Nf2^{f/f}$, $Cdkn2a^{f/f}$, $Bap1^{f/f}$;$Nf2^{f/f}$, $Bap1^{f/f}$;$Cdkn2a^{f/f}$, $Nf2^{f/f}$;$Cdkn2a^{f/f}$, and $Bap1^{f/f}$;$Nf2^{f/f}$;$Cdkn2a^{f/f}$ mice. The mesothelial cells were then exposed to either control Adeno-CMV or Adeno-Cre virus for 1 h, seeded in non-adherent plates in serum-free stem cell medium (21), and photographed after 9 days. There was little or no evidence of spheroid formation in cultured WT mesothelial cells or mesothelial cells with Adeno-Cre-induced homozygous inactivation of one or various combinations of two tumor suppressor genes (representative examples shown in Figure 5). In contrast, Adeno-Cre-treated mesothelial cells from

Bap1$^{f/f}$;*Nf2*$^{f/f}$;*Cdkn2a*$^{f/f}$ mice, i.e., with inactivation of all three MM driver genes, showed multiple large spheroids, indicative of stem cell features (Figure 5).

RNA-seq analysis of MMs from triple-CKO mice reveals enrichment of genes transcriptionally regulated by the polycomb repressive complex 2 (PRC2)

Given the striking shift in MM latency between *Bap1*;*Nf2*;*Cdkn2a* CKO mice and *Nf2*;*Cdkn2a* CKO mice, as well as the consistently more aggressive nature of MMs from triple-CKO (TKO) mice, we performed RNA-seq analysis on MMs from these two cohorts to shed light on the contribution of *Bap1* inactivation in this experimental setting. This analysis was carried out on all 6 MMs from *Bap1*;*Nf2*;*Cdkn2a* CKO mice shown in Figure 4 versus 2 MMs from *Nf2*;*Cdkn2a* CKO mice in which Bap1 expression was retained (tumors 375 and 411 in Figure 4). Among 1,425 genes identified as differentially expressed with fold-change of at least 2 and false discovery rate (FDR) <1%, significantly fewer genes (628, 44%) were upregulated than downregulated (p-value = 8.4×10^{-6}, exact binomial test) in MMs from *Bap1*-deficient TKO mice versus *Bap1*-expressing MMs from DKO mice. Functional enrichment analysis with GSEA identified several highly significant (family-wise error rate < 0.0005) curated gene sets. Prominent among the positively enriched gene sets were those related to writers of histone H3K27Me3, including PRC2 and SUZ12 (Figure 6A), as well as genes participating in cell proliferation and transcription regulation involving ubiquitin signaling mediated by the Bap1-HCF1-YY1 complex, EED-related stem cell pluripotency, cytokine signaling, and cell adhesion; 100 of the top pathways differentially affected in MMs from TKO versus DKO mice are presented in Supplemental Table 3. Considering that Bap1 plays an important role in chromatin remodeling and transcriptional regulation (23–25), and the fact that many of the top differentially expressed genes were significantly enriched for PRC2 target genes (40), we decided to focus further on PRC2 targets here. A heatmap of genes differentially expressed in MMs from triple-CKO mice versus MMs from *Nf2*;*Cdkn2a* double-CKO mice is shown in Figure 6B. Thirteen cancer-related genes were validated by RT-PCR analysis, 6 of which (e.g., *Ptchd1* and *Diras1*) are depicted in Figure 6C and Supplemental Figure 3. Mmp9 protein was also shown to be overexpressed and activated in MMs from TKO mice versus those from DKO mice (Figure 6D).

Discussion

In this investigation, our aim was to induce mesothelial cell-specific homozygous deletions of three tumor suppressor genes (*Bap1*, *Nf2*, and *Cdkn2a*) that have been implicated as major drivers of human MM pathogenesis. While the majority of malignant tumors observed were MMs, additional tumor types also resulted, possibly due to infection of other intrathoracic tissues or by passage of virus via blood vessels to the liver. Notably, HCCs and ICCs were very common later in life in *Bap1;Nf2* CKO mice but were observed in only two CKO mice with any of the other genotypes. Notably, liver-specific deletion of *Nf2* in the developing or adult mouse has been reported to promote a marked, progressive expansion of progenitor cells throughout the liver, with all surviving mice eventually developing both HCC and ICC (41). Interestingly, HCC and ICC were not seen in our *Bap1;Nf2;Cdkn2a*

CKO cohort, perhaps because these mice succumbed to MM before hepatic tumors could be detected.

Overall, the MMs observed in our GEM cohorts generally showed morphological features, immunohistochemical staining, and invasiveness similar to that of human sarcomatoid MMs, with the exception being those observed in *Bap1;Nf2* CKO mice, in which 6 of 7 MMs showed mixed (biphasic) histology that also was similar histologically to their human biphasic counterparts.

The Kaplan-Meier curves (Figure 2B) indicate that homozygous inactivation of different combinations of *Bap1*, *Nf2*, and *Cdkn2a* affect MM latency differently, with losses of all three genes profoundly accelerating tumor development. Specifically, *Bap1;Nf2;Cdkn2a* CKO mice bearing MM showed much shorter tumor latency than mice in any compound double-CKO cohort. Moreover, MMs from triple-CKO mice consistently appeared to be high grade, very invasive, hypercellular tumors whereas MMs from mice with other genotypes were more variable phenotypically. All MMs observed in our study were sarcomatoid or biphasic, similar to what was reported by Jongsma et al. for mice with homozygously floxed conditional compound alleles that were injected IT with Adeno-Cre (20). For example, in their *Nf2;Cdkn2a* CKO mice, 31 MMs were sarcomatoid, 13 had mixed histology, and only 1 was epithelioid (20). These investigators had speculated that the predominant epithelioid histology seen in human MMs, as opposed to mice, may be the result of species-specific differences or route of induction, including the long latency and exposure to asbestos in the human disease counterpart (20). It is also likely that the particular mouse strain can influence the phenotype observed. For example, in our previous asbestos carcinogenesis work, $Nf2^{+/-}$ mice in a 129Sv/Jae genetic background injected intraperitoneally (IP) with asbestos developed roughly equivalent percentages of epithelioid, mixed, and sarcomatoid MMs (4), whereas asbestos-injected $Nf2^{+/-}$ mice in a FVB/N background mostly developed sarcomatoid MMs (21).

Heterozygous knockout ($^{+/-}$) and heterozygous mutant (+/mut) *Bap1* mice injected IP with asbestos exhibit a highly significant increase in the incidence of MMs as compared to asbestos-injected WT littermates, providing *in vivo* evidence that *Bap1* inactivation plays an important role in MM tumorigenesis (30,31). Similarly, heterozygous *Nf2* mice injected with asbestos develop MM with a markedly shorter latency than asbestos-treated WT littermates (4,19). Heterozygous *Cdkn2a* knockout mice treated with asbestos also develop MM at an accelerated rate compared to asbestos-treated WT mice (14). Furthermore, asbestos-exposed compound $Nf2^{+/-};Cdkn2a^{+/-}$ mice show further acceleration of asbestos-induced MM and increased presence of cancer stem cells (21). These carcinogenesis studies, in combination with the gene knockout model studies reported here strongly support a working hypothesis that *Bap1*, *Nf2*, and *Cdkn2a* are key drivers of MM pathogenesis and that the collective losses of these three tumor suppressors is sufficient to drive rapidly disseminated, lethal disease, similar to the poor clinical outcome of human pleural MM.

In one study, CKO mice in which only one of these tumor suppressor genes was homozygously deleted developed MM at a low rate, with spontaneous MM-like tumors being identified in 5 of 30 $Nf2^{f/f}$ mice and 0/17 $Cdkn2a^{f/f}$ mice injected IT with Adeno-Cre

(20), supporting the notion that MM development requires the combined involvement of multiple tumor suppressor gene alterations (42). Similarly, in our *Bap1* CKO cohort, MM was seen in only 1 of 32 mice. The fact that MM arises spontaneously in a considerable number of CKO mice made deficient for both alleles of two or more tumor suppressor genes, provides compelling support for the role of genetics in MM causation and the need for accumulated genetic and epigenetic alterations for tumor formation (1). As an example, even in the one *Bap1* CKO mouse that did develop MM, it is intriguing that there was acquired loss of Nf2 and p16Ink4a expression during tumorigenesis.

The *in vivo* findings presented here with CKO mice closely mimic those found in the human disease counterpart, in which losses of *BAP1*, *CDKN2A*, and *NF2* are frequently seen in various combinations (7,43). Their frequent occurrence in MM and their individual roles both in various cancer predisposition syndromes and in tumor progression strongly suggest that they are key drivers in MM pathogenesis. Our initial work on *BAP1* provided the first demonstration that genetics influences the risk of MM, a cancer linked to mineral fiber carcinogenesis (8). However, there is evidence that germline mutations of *CDKN2A* and *NF2* may also modulate susceptibility to mineral fiber carcinogens. For example, Betti et al. recently described a family in which both MM and cutaneous melanoma cases were found to have a deleterious germline missense mutation in the *CDKN2A* gene, and the family member with MM was determined to be of the low exposure category (44). Additionally, germline mutations in *NF2* have been reported in patients who developed MM. In one case, an individual with neurofibromatosis, type II (NF2) developed peritoneal MM at the relatively young age of 40 (45). Comparative genomic hybridization analysis and IHC staining of the MM tissue revealed loss of the *NF2* gene and protein product, respectively. A second NF2 patient developed a pleural MM at age 75 (46). Both patients were reported to have occupational asbestos exposure.

Our observation that CKO mice with losses of all three tumor suppressor genes had much higher MM penetrance and markedly shorter survival than mice with loss of one or two of these genes fits with the model put forward by Vogelstein and Kinzler (47). They proposed that in solid tumors of adults, alterations in a minimum of three mutated driver genes are needed for a cell to evolve into an invasive (malignant) tumor. In our CKO models, loss of one or two tumor suppressors was not consistently sufficient to result in a high incidence of MMs. The exception was the *Nf2;Cdkn2a* CKO model, but even in these mice tumor latency was much longer than in the triple-CKO mouse model. One possibility is that in *Nf2;Cdkn2a* CKO mice, significantly more time is needed in order to accumulate additional genetic and epigenetic alterations sufficient to result in an invasive cancer. In fact, 4 of 6 MMs tested from *Nf2;Cdkn2a* CKO mice acquired loss of Bap1 expression (Figure 4), suggesting that Bap1 loss may be favored in the progression of these tumors. In human MM, tumors are characterized by the presence of multiple somatic genetic and cell signaling alterations. The fact that large spheroids can be reproducibly formed *in vitro* in normal mesothelial cells following Adeno-Cre-induced excision of *Bap1*, *Cdkn2a* and *Nf2*, but not by the excision of only one or two of these genes, also provides experimental support for cooperativity between the inactivation of these three tumor suppressor genes in MM tumorigenesis.

Our RNA-seq analysis revealed that MMs from *Bap1*;*Nf2*;*Cdkn2a* CKO mice exhibit positively enriched gene sets consistent with cellular processes previously implicated in Bap1 function, such as genes mediated by the Bap1-HCF1-YY1 complex, which play a role in cellular proliferation and transcription regulation involving ubiquitin signaling (25). In addition, in the experimental context used here, we have uncovered a connection between Bap1 and PRC2 that has been less well established than other previously reported Bap1-related cellular activities.

Interestingly, a considerable number of upregulated genes in MMs from triple-CKO mice have been implicated as oncogenes or pro-invasion/metastasis genes, whereas several tumor suppressor genes were downregulated. Lafave et al. demonstrated that BAP1 inactivation leads to EZH2-dependent transformation (48). Although their report did not include RNA-seq analysis on human MM tumors for comparison with our murine data, they demonstrated that *BAP1*-deficient MM cells are sensitive to EZH2 pharmacologic inhibition, and our findings add support to their conclusion that such an approach may have clinical efficacy. It is noteworthy that PRC2 subunits such as Ezh2 have been shown to have context-dependent oncogenic or tumor suppressive roles in different cancers (49).

To investigate if our CKO mouse model findings are recapitulated in human MMs with biallelic inactivation of *BAP1*, *CDKN2A* and *NF2* versus MMs with biallelic inactivation of *CDKN2A* and *NF2* only, we analyzed data from The Cancer Genome Atlas (TCGA) (Supplemental Materials and Methods; Figure 6E, F). GSEA analysis of the TCGA data revealed several positively enriched gene sets associated with SUZ12, PRC2, as well as EZH2 mediated tri-methylation of H3K27 in human MMs with biallelic inactivation of all three tumor suppressor genes (Figure 6F; Supplemental Table 4), similar to the situation in MMs from our TKO mice.

Mechanistically, our findings suggest that losses of *Bap1*, *Nf2* and *Cdkn2a* cooperate by disrupting multiple cellular pathways that lead to the transformation of normal mesothelial cells to MM cells. Thus, *Cdkn2a* loss would result in insensitivity to antigrowth signals (via p16Ink4a loss) and evasion of apoptosis (p19Arf loss), whereas *Nf2* loss would be expected to result in evasion of apoptosis and tissue invasion/metastasis (Hippo, Pak) and TAZ-related MM cell transformation and transcriptional induction of distinct pro-oncogenic genes, including cytokines (50). Based on the upregulated genes identified in MMs from TKO mice, other possible effects such as Lmo1-induced ECM and integrin-related self-sufficiency in growth signals, Aldh1a2- and Gli1-related maintenance of cancer stem cells, and Mmp9-induced invasiveness (Figure 6D) may be mechanistically connected with Bap1 inactivation and will be explored in future studies.

Collectively, $Bap1^{f/f};Nf2^{f/f};Cdkn2a^{f/f}$ mice injected IT with Adeno-Cre appear to be useful for modeling an aggressive form of MM. These MMs develop at a high incidence after a short latency period. Moreover, our finding that loss of *Bap1* contributes to MM pathogenesis, in part, via loss of PRC2-mediated gene repression of certain oncogenic target genes, suggests a potential avenue for therapeutic intervention that may be rapidly tested in this CKO model.

Supplementary Material

Refer to Web version on PubMed Central for supplementary material.

Acknowledgments

Grant Support

This work was supported by NCI grants CA175691 (to J.R. Testa and F.J. Rauscher III) and CA06927 (to FCCC) and an appropriation from the Commonwealth of Pennsylvania to FCCC. Other support was provided by the Local #14 Mesothelioma Fund of the International Association of Heat and Frost Insulators and Allied Workers. We thank Emmanuelle Nicolas for RT-PCR analyses, Eric Ross for statistical assistance, Alfonso Bellacosa for critical reading of the manuscript, and Raza Zaidi, Xavier Graña, Siddharth Balachandran, and Richard Pomerantz for scientific advice and technical suggestions. The following FCCC core services assisted this project: Laboratory Animal, Transgenic Mouse, Genomics, Cell Culture, DNA Sequencing, Histopathology, and Biostatistics and Bioinformatics Facilities.

References

1. Murthy SS, Testa JR. Asbestos, chromosomal deletions, and tumor suppressor gene alterations in human malignant mesothelioma. J Cell Physiol 1999;180:150–7. [PubMed: 10395284]
2. Cheng JQ, Jhanwar SC, Klein WM, Bell DW, Lee W-C, Altomare DA, et al. *p16* alterations and deletion mapping of 9p21-p22 in malignant mesothelioma. Cancer Res 1994;54:5547–51. [PubMed: 7923195]
3. Xio S, Li D, Vijg J, Sugarbaker DJ, Corson JM, Fletcher JA. Codeletion of p15 and p16 in primary malignant mesothelioma. Oncogene 1995;11:511–5. [PubMed: 7630635]
4. Altomare DA, Vaslet CA, Skele KL, De Rienzo A, Devarajan K, Jhanwar SC, et al. A mouse model recapitulating molecular features of human mesothelioma. Cancer Res 2005;65:8090–5. [PubMed: 16166281]
5. Sekido Y, Pass HI, Bader S, Mew DJY, Christman MF, Gazdar AF, et al. Neurofibromatosis type 2 (*NF2*) gene is somatically mutated in mesothelioma but not in lung cancer. Cancer Res 1995;55:1227–31. [PubMed: 7882313]
6. Bianchi AB, Mitsunaga S-I, Cheng JQ, Klein WM, Jhanwar SC, Seizinger B, et al. High frequency of inactivating mutations in the neurofibromatosis type 2 gene (*NF2*) in primary malignant mesotheliomas. Proc Natl Acad Sci U S A 1995;92:10854–8. [PubMed: 7479897]
7. Bott M, Brevet M, Taylor BS, Shimizu S, Ito T, Wang L, et al. The nuclear deubiquitinase BAP1 is commonly inactivated by somatic mutations and 3p21.1 losses in malignant pleural mesothelioma. Nat Genet 2011;43:668–72. [PubMed: 21642991]
8. Testa JR, Cheung M, Pei J, Below JE, Tan Y, Sementino E, et al. Germline BAP1 mutations predispose to malignant mesothelioma. Nat Genet 2011;43:1022–5. [PubMed: 21874000]
9. Hmeljak J, Sanchez-Vega F, Hoadley KA, Shih J, Stewart C, Heiman D, et al. Integrative molecular characterization of malignant pleural mesothelioma. Cancer Discov 2018;8:1548–65. [PubMed: 30322867]
10. Cheng JQ, Lee WC, Klein MA, Cheng GZ, Jhanwar SC, Testa JR. Frequent mutations of *NF2* and allelic loss from chromosome band 22q12 in malignant mesothelioma: evidence for a two-hit mechanism of NF2 inactivation. Genes Chromosomes Cancer 1999;24:238–42. [PubMed: 10451704]
11. Nasu M, Emi M, Pastorino S, Tanji M, Powers A, Luk H, et al. High incidence of somatic *BAP1* alterations in sporadic malignant mesothelioma. J Thoracic Oncol 2015;10:565–76.
12. Frizelle SP, Grim J, Zhou J, Gupta P, Curiel DT, Geradts J, et al. Re-expression of p16INK4a in mesothelioma cells results in cell cycle arrest, cell death, tumor suppression and tumor regression. Oncogene 1998;16:3087–95. [PubMed: 9671387]
13. Yang CT, You L, Yeh CC, Chang JW, Zhang F, McCormick F, et al. Adenovirus-mediated p14(ARF) gene transfer in human mesothelioma cells. J Natl Cancer Inst 2000;92:636–41. [PubMed: 10772681]

14. Altomare DA, Menges CW, Xu J, Pei J, Zhang L, Tadevosyan A, et al. Losses of both products of the *Cdkn2a/Arf* locus contribute to asbestos-induced mesothelioma development and cooperate to accelerate tumorigenesis. PLoS One 2011;6:e18828. [PubMed: 21526190]
15. Xiao GH, Gallagher R, Shetler J, Skele K, Altomare DA, Pestell RG, et al. The *NF2* tumor suppressor gene product, merlin, inhibits cell proliferation and cell cycle progression by repressing cyclin D1 expression. Mol Cell Biol 2005;25:2384–94. [PubMed: 15743831]
16. Lopez-Lago MA, Okada T, Murillo MM, Socci N, Giancotti FG. Loss of the tumor suppressor gene *NF2*, encoding merlin, constitutively activates integrin-dependent mTORC1 signaling. Mol Cell Biol 2009;29:4235–49. [PubMed: 19451229]
17. Xiao GH, Beeser A, Chernoff J, Testa JR. p21-activated kinase links Rac/Cdc42 signaling to merlin. J Biol Chem 2002;277:883–6. [PubMed: 11719502]
18. Poulikakos PI, Xiao GH, Gallagher R, Jablonski S, Jhanwar SC, Testa JR. Re-expression of the tumor suppressor NF2/merlin inhibits invasiveness in mesothelioma cells and negatively regulates FAK. Oncogene 2006;25:5960–8. [PubMed: 16652148]
19. Fleury-Feith J, Lecomte C, Renier A, Matrat M, Kheuang L, Abramowski V, et al. Hemizygosity of *Nf2* is associated with increased susceptibility to asbestos-induced peritoneal tumours. Oncogene 2003;22:3799–805. [PubMed: 12802287]
20. Jongsma J, van Montfort E, Vooijs M, Zevenhoven J, Krimpenfort P, van der Valk M, et al. A conditional mouse model for malignant mesothelioma. Cancer Cell 2008;12:261–71.
21. Menges CW, Kadariya Y, Altomare D, Talarchek J, Neumann-Domer E, Wu Y, et al. Tumor suppressor alterations cooperate to drive aggressive mesotheliomas with enriched cancer stem cells via a p53-miR-34a-c-Met axis. Cancer Res 2014;74:1261–71. [PubMed: 24371224]
22. Jensen DE, Proctor M, Marquis ST, Gardner HP, Ha SI, Chodosh LA, et al. BAP1: a novel ubiquitin hydrolase which binds to the BRCA1 RING finger and enhances BRCA1-mediated cell growth suppression. Oncogene 1998;16:1097–112. [PubMed: 9528852]
23. Scheuermann JC, de Ayala Alonso AG, Oktaba K, Ly-Hartig N, McGinty RK, Fraterman S, et al. Histone H2A deubiquitinase activity of the Polycomb repressive complex PR-DUB. Nature 2010;465:243–7. [PubMed: 20436459]
24. Misaghi S, Ottosen S, Izrael-Tomasevic A, Arnott D, Lamkanfi M, Lee J, et al. Association of C-terminal ubiquitin hydrolase BRCA1-associated protein 1 with cell cycle regulator host cell factor 1. Mol Cell Biol 2009;29:2181–92. [PubMed: 19188440]
25. Yu H, Mashtalir N, Daou S, Hammond-Martel I, Ross J, Sui G, et al. The ubiquitin carboxyl hydrolase BAP1 forms a ternary complex with YY1 and HCF-1 and is a critical regulator of gene expression. Mol Cell Biol 2010;30:5071–85. [PubMed: 20805357]
26. Yu H, Pak H, Hammond-Martel I, Ghram M, Rodrigue A, Daou S, et al. Tumor suppressor and deubiquitinase BAP1 promotes DNA double-strand break repair. Proc Natl Acad Sci U S A 2014;111:285–90. [PubMed: 24347639]
27. Baughman JM, Rose CM, Kolumam G, Webster JD, Wilkerson EM, Merrill AE, et al. NeuCode proteomics reveals Bap1 regulation of metabolism. Cell Rep 2016;16:583–95. [PubMed: 27373151]
28. Gezgin G, Dogrusoz M, van Essen TH, Kroes WGM, Luyten GPM, van der Velden PA, et al. Genetic evolution of uveal melanoma guides the development of an inflammatory microenvironment. Cancer Immunol Immunother 2017;66:903–12. [PubMed: 28391358]
29. Affar EB, Carbone M. BAP1 regulates different mechanisms of cell death. Cell Death Dis 2018;9:1151. [PubMed: 30455474]
30. Xu J, Kadariya Y, Cheung M, Pei J, Talarchek J, Sementino E, et al. Germline mutation of *Bap1* accelerates development of asbestos-induced malignant mesothelioma. Cancer Res 2014;74:4388–97. [PubMed: 24928783]
31. Napolitano A, Pellegrini L, Dey A, Larson D, Tanji M, Flores EG, et al. Minimal asbestos exposure in germline *BAP1* heterozygous mice is associated with deregulated inflammatory response and increased risk of mesothelioma. Oncogene 2016;35:1996–2002. [PubMed: 26119930]

32. Baumann F, Flores E, Napolitano A, Kanodia S, Taioli E, Pass H, et al. Mesothelioma patients with germline *BAP1* mutations have 7-fold improved long-term survival. Carcinogenesis 2015;36:76–81. [PubMed: 25380601]
33. Ohar JA, Cheung M, Talarchek J, Howard SE, Howard TD, Hesdorffer M, et al. Germline BAP1 Mutational landscape of asbestos-exposed malignant mesothelioma patients with family history of cancer. Cancer Res 2016;76:206–15. [PubMed: 26719535]
34. Harbour JW, Onken MD, Roberson ED, Duan S, Cao L, Worley LA, et al. Frequent mutation of *BAP1* in metastasizing uveal melanomas. Science 2010;330:1410–3. [PubMed: 21051595]
35. Pena-Llopis S, Vega-Rubin-de-Celis S, Liao A, Leng N, Pavia-Jimenez A, Wang S, et al. *BAP1* loss defines a new class of renal cell carcinoma. Nat Genet 2012;44:751–9. [PubMed: 22683710]
36. Bot J, Whitaker D, Vivian J, Lake R, Yao V, McCauley R. Culturing mouse peritoneal mesothelial cells. Pathol Res Pract 2003;199:341–4. [PubMed: 12908525]
37. Love MI, Huber W, Anders S. Moderated estimation of fold change and dispersion for RNA-seq data with DESeq2. Genome Biol 2014;15:550. [PubMed: 25516281]
38. Durinck S, Spellman PT, Birney E, Huber W. Mapping identifiers for the integration of genomic datasets with the R/Bioconductor package biomaRt. Nat Protoc 2009;4:1184–91. [PubMed: 19617889]
39. Subramanian A, Tamayo P, Mootha VK, Mukherjee S, Ebert BL, Gillette MA, et al. Gene set enrichment analysis: a knowledge-based approach for interpreting genome-wide expression profiles. Proc Natl Acad Sci U S A 2005;102:15545–50. [PubMed: 16199517]
40. Sashida G, Wang C, Tomioka T, Oshima M, Aoyama K, Kanai A, et al. The loss of Ezh2 drives the pathogenesis of myelofibrosis and sensitizes tumor-initiating cells to bromodomain inhibition. The J Exp Med 2016;213:1459–77. [PubMed: 27401345]
41. Benhamouche S, Curto M, Saotome I, Gladden AB, Liu CH, Giovannini M, et al. Nf2/Merlin controls progenitor homeostasis and tumorigenesis in the liver. Genes Dev 2010;24:1718–30. [PubMed: 20675406]
42. Taguchi T, Jhanwar SC, Siegfried JM, Keller SM, Testa JR. Recurrent deletions of specific chromosomal sites in 1p, 3p, 6q, and 9p in human malignant mesothelioma. Cancer Res 1993;53:4349–55. [PubMed: 8364929]
43. Cheung M, Testa JR. *BAP1*, a tumor suppressor gene driving malignant mesothelioma. Transl Lung Cancer Res 2017;6:270–8. [PubMed: 28713672]
44. Betti M, Aspesi A, Biasi A, Casalone E, Ferrante D, Ogliara P, et al. *CDKN2A* and *BAP1* germline mutations predispose to melanoma and mesothelioma. Cancer Lett 2016;378:120–30. [PubMed: 27181379]
45. Baser ME, De Rienzo A, Altomare D, Balsara BR, Hedrick NM, Gutmann DH, et al. Neurofibromatosis 2 and malignant mesothelioma. Neurology 2002;59:290–1. [PubMed: 12136076]
46. Baser ME, Rai H, Wallace AJ, Evans DG. Neurofibromatosis 2 (NF2) and malignant mesothelioma in a man with a constitutional *NF2* missense mutation. Fam Cancer 2005;4:321–2. [PubMed: 16341811]
47. Vogelstein B, Kinzler KW. The path to cancer — three strikes and you're out. N Engl J Med 2015;373:1895–8. [PubMed: 26559569]
48. LaFave LM, Beguelin W, Koche R, Teater M, Spitzer B, Chramiec A, et al. Loss of BAP1 function leads to EZH2-dependent transformation. Nat Med 2015;21:1344–9. [PubMed: 26437366]
49. Vo BT, Li C, Morgan MA, Theurillat I, Finkelstein D, Wright S, et al. Inactivation of Ezh2 upregulates Gfi1 and drives aggressive Myc-driven group 3 medulloblastoma. Cell Rep 2017;18:2907–17. [PubMed: 28329683]
50. Matsushita A, Sato T, Mukai S, Fujishita T, Mishiro-Sato E, Okuda M, et al. TAZ activation by Hippo pathway dysregulation induces cytokine gene expression and promotes mesothelial cell transformation. Oncogene 2019;38:1966–78. [PubMed: 30401981]

Significance:

Combinatorial deletions of *Bap1*, *Nf2* and *Cdkn2a* result in aggressive mesotheliomas, with *Bap1* loss contributing to tumorigenesis by circumventing PRC2-mediated repression of oncogenic target genes.

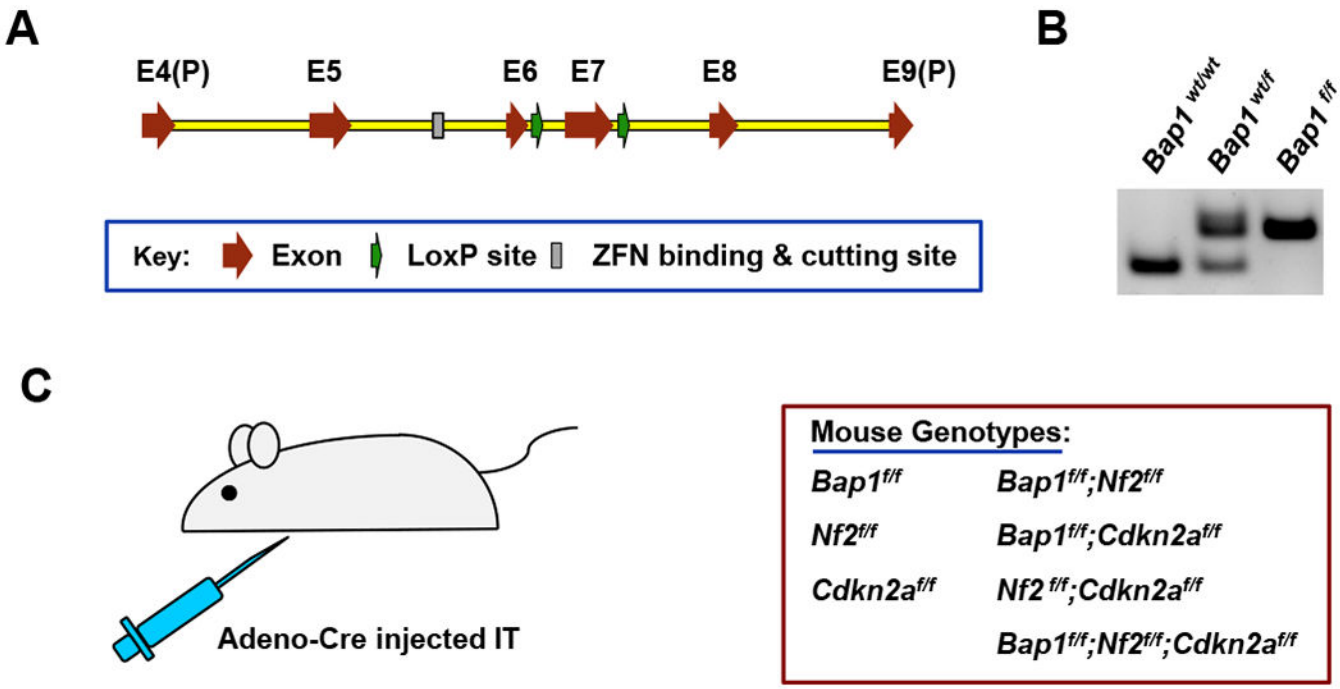

Figure 1.

Generation of *Bap1* conditional knockout (CKO) mouse with zinc finger nuclease (ZFN) technology, and experimental schema used for crosses with other CKO mice. **A,** Schematic drawing of *Bap1* LoxP donor DNA sequence. Donor DNA contains region spanning part of exon 4, E4(P), to part of exon 9, E9(P). LoxP sites were inserted into introns 6 and 7. A pair of ZFNs was identified that binds to and cuts within a site in intron 5 of *Bap1* with high efficiency and specificity. A donor DNA construct was then designed that contained two LoxP sites, one in intron 6 and one in intron 7, as shown, such that expression of Adeno-Cre in the mouse mesothelial cell lining the pleural cavity excises exon 7 of *Bap1*. **B,** Genotyping of DNA from wild type (wt) mouse as well as heterozygous (wt/f) and homozygous (f/f) *Bap1* CKO mice. **C,** Strategy used to homozygously excise *Bap1*, *Nf2*, and/or *Cdkn2a* via intrathoracic (IT) injection of Adeno-Cre virus in mice with the various genotypes shown.

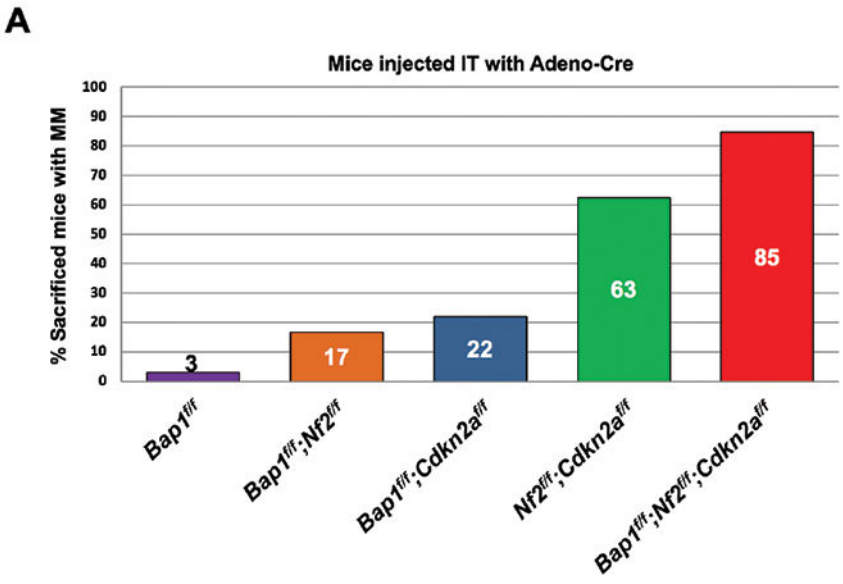

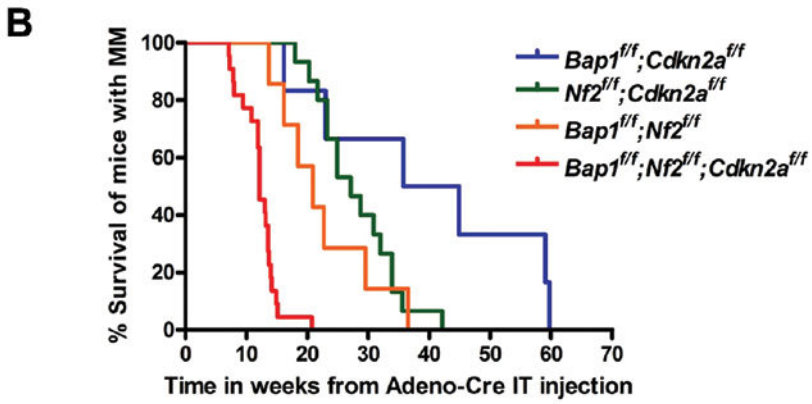

Genotype	% Mice with MM	Median survival in weeks
Bap1$^{f/f}$;*Cdkn2a*$^{f/f}$	6 / 27 (22%)	40
Bap1$^{f/f}$;*Nf2*$^{f/f}$	7 / 42 (17%)	21
Nf2$^{f/f}$;*Cdkn2a*$^{f/f}$	15 / 24 (63%)	27
Bap1$^{f/f}$;*Nf2*$^{f/f}$;*Cdkn2a*$^{f/f}$	22 / 26 (85%)	12

Figure. 2.

Incidence and latency of pleural malignant mesothelioma (MM) in mouse cohorts with different genotypes following intrathoracic (IT) injections with Adeno-Cre virus. **A,** Incidence of MM in the various CKO mouse groups. **B,** Tumor latency curves for MMs arising after Adeno-Cre injections in mice with CKO of different combinations of *Bap1*, *Nf2* and/or *Cdkn2a*. Kaplan-Meier curves depict survival of mice succumbing to MM arising after IT injections with Adeno-Cre. Note rapid development of MM in triple-CKO mice, with the median survival being only 12 weeks, which was significantly different ($p<0.0001$)

from that of any of the other compound CKO mice. The survival differences between the other three double knockout (DKO) mouse cohorts were not statistically significant (Supplemental Table 2).

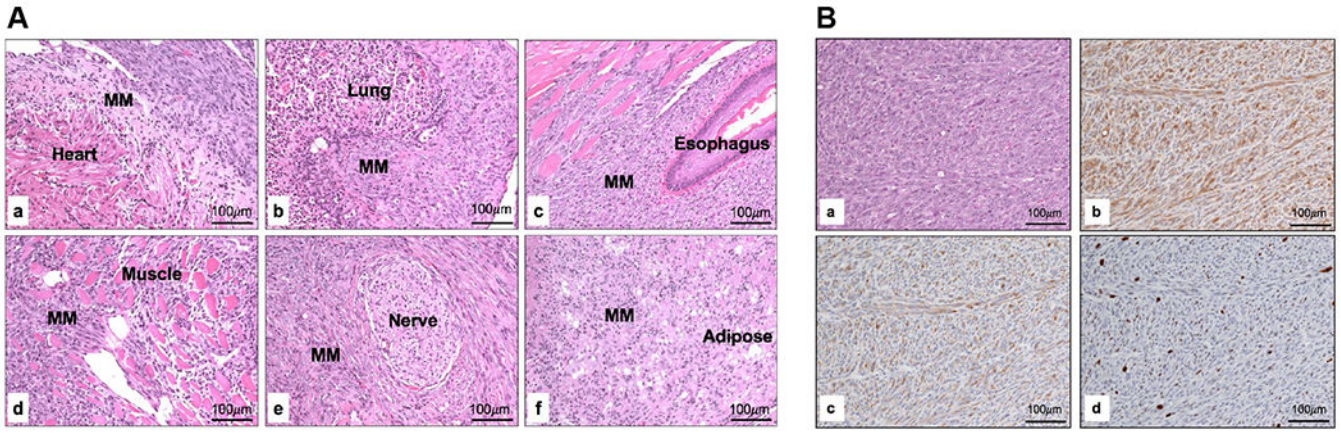

Figure 3.

Histopathological assessment of representative high-grade MMs from *Bap1;Nf2;Cdkn2a* CKO mice. **A,** Histopathology of highly invasive, disseminated MM that arose in a *Bap1;Nf2;Cdkn2a* CKO mouse following IT injection of Adeno-Cre. Note MM invasion affecting multiple organs including the heart (a), lung (b), esophagus (c), skeletal muscle (d), nerve (e), and mediastinal adipose tissue (f). **B,** Serial sections of a MM from a *Bap1;Nf2;Cdkn2a* CKO mouse showing H&E staining (a), and IHC for mesothelin (b), cytokeratin 8 marker TROMA-1 (c), and nuclear proliferation marker Ki-67 (d).

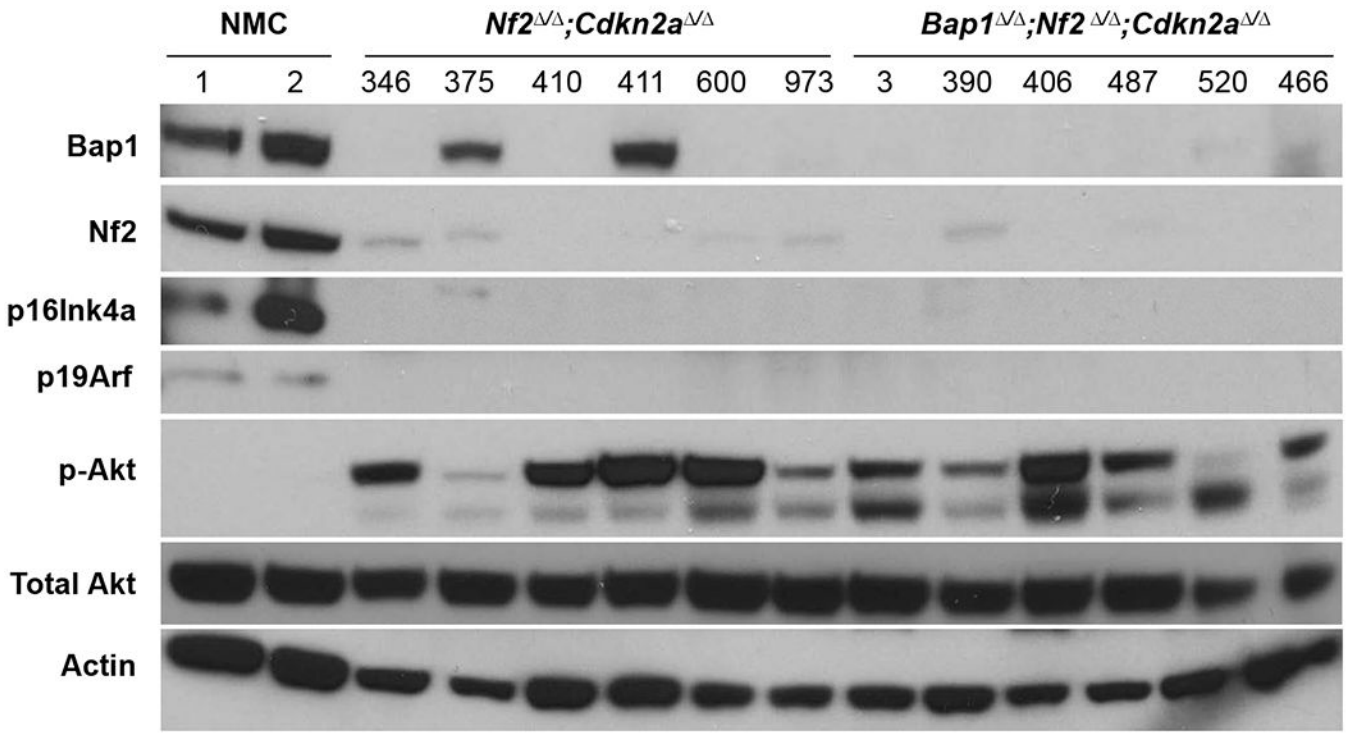

Figure 4.

Western blot analysis of normal mesothelial cells (NMC) and MMs from *Nf2;Cdkn2a* double-knockout (DKO) and *Bap1;Nf2;Cdkn2a* triple-knockout (TKO) mice. Immunoblots confirm loss of expression of proteins encoded by conditionally knocked out genes *Bap1*, *Nf2* and *Cdkn2a* (p16Ink4a and p19Arf) in all tumors. Acquired loss of expression of Bap1 was also observed in 4 of 6 MMs from *Nf2;Cdkn2a* DKO mice. Interestingly, this acquired loss of Bap1 expression appears to have occurred at the post-translational level, as these tumors showed no *Bap1* mutations, deletions, or loss of mRNA expression. Phosphorylated Akt, indicative of Akt activation, is seen in all MMs shown.

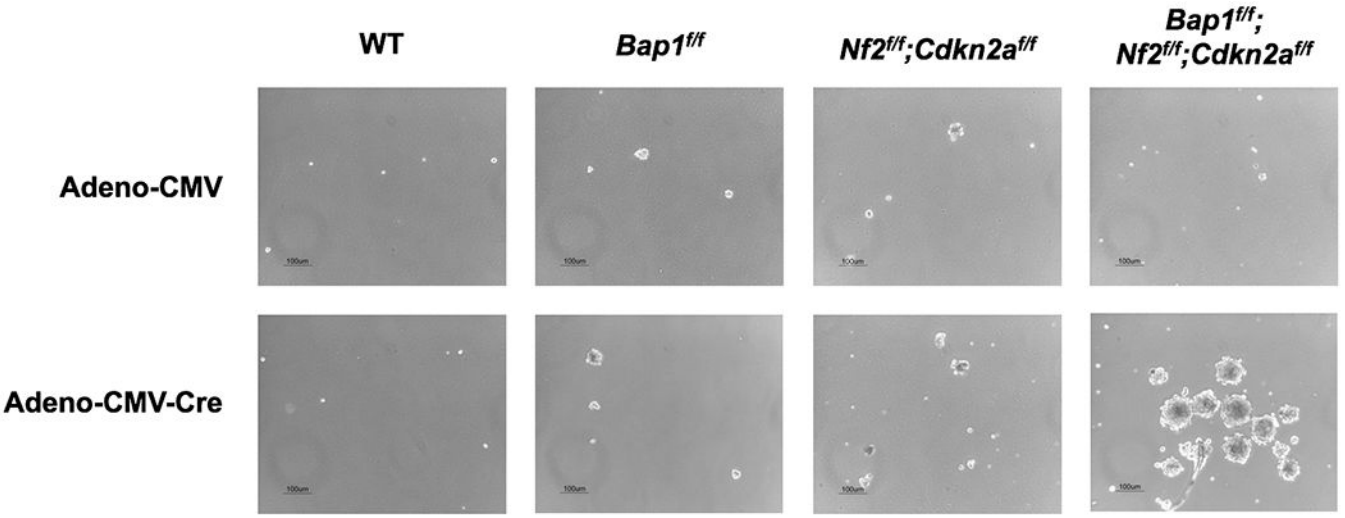

Figure 5.

Ad5CMVCre virus-exposed normal mesothelial cells (NMC) from *Bap1*$^{f/f}$;*Nf2*$^{f/f}$;*Cdkn2a*$^{f/f}$ mice harbor more and much larger stem cell-like spheroids than do those from wild-type (WT), *Bap1*$^{f/f}$, and *Nf2*$^{f/f}$;*Cdkn2a*$^{f/f}$ mice. Equal numbers of NMC from mice with the various cited genotypes were seeded on non-adherent 6-well plates in stem cell media, and spheroids were photographed after 9 days.

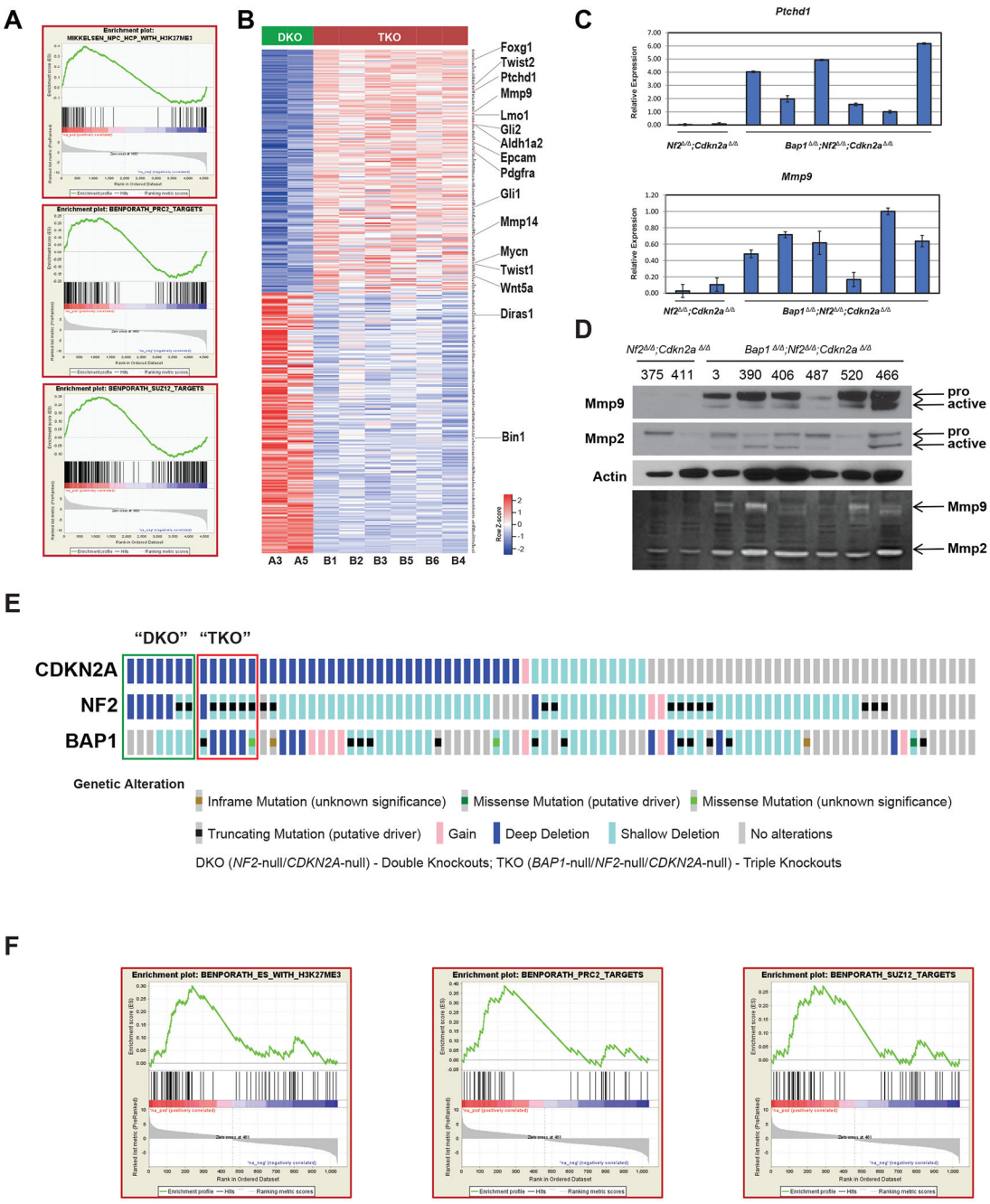

Figure 6.

Heatmap and GSEA of same MMs (B1-B6) from *Bap1;Nf2;Cdkn2a* triple-knockout (TKO) mice shown in Figure 4 versus two MMs, A3 and A5 (375 and 411, respectively), from *Nf2;Cdkn2a* double knockout (DKO) mice retaining expression of Bap1. **A,** Gene enrichment plots of several gene sets differentially expressed in MMs from TKO versus DKO mice. **B,** Top 400 PRC2 target genes differentially expressed with at least 2-fold change and FDR of <1%. Genes are ranked by significance, with most significantly upregulated PRC2 target at top and most significantly downregulated at bottom. A number

of the indicated upregulated genes have been implicated in oncogenesis, cancer cell stemness, pro-invasion/metastasis, adhesion, and cytokine and/or hedgehog signaling, and two downregulated genes (*Bin1*, *Diras1*) encode tumor suppressors. **C,** RT-PCR analysis was performed on 13 of the 16 indicated genes (2 shown here), validating the RNA-seq data in each instance. **D,** Immunoblot demonstrating overexpression of Mmp9 and Mmp2 in MMs from TKO mice (upper panel). Upper bands indicate respective pro-Mmp9 and pro-Mmp2; lower bands represent cleaved, active forms. Lysates were run on Novex 10% Zymogram gel and stained using colloidal blue staining kit to visualize Mmp2/9 activity (lower panel). **E,** Assessment of *BAP1*, *CDKN2A* and *NF2* in 87 human MMs from TCGA. Seven MMs (green open rectangle, designated DKO here) were null for both *CDKN2A* and *NF2*, and 6 (red open rectangle, designated TKO) were null for *BAP1*, *CDKN2A* and *NF2*. **F,** Gene enrichment plots of several gene sets differentially expressed in TKO versus DKO MMs.

Table 1.

Summary of tumors observed in homozygous conditional knockout (CKO) mice arising after intrathoracic (IT) injection of Adeno-Cre.

Genotype[a]	*Bap1*$^{f/f}$	*Bap1*$^{f/f}$; *Nf2*$^{f/f}$	*Bap1*$^{f/f}$; *Cdkn2a*$^{f/f}$	*Nf2*$^{f/f}$; *Cdkn2a*$^{f/f}$	*Bap1*$^{f/f}$;*Nf2*$^{f/f}$; *Cdkn2a*$^{f/f}$
No. mice injected	32	42	27	24	26
MM[b]	1 (3.1%)	7[c] (16.6%)	6 (22.2%)	15[d] (62.5%)	22 (84.6%)
Epithelioid	0	0	0	0	0
Mixed (Biphasic)	0	6	1	4	8
Sarcomatoid	1	1	5	11	14
Lymphoma	1	0	0	0	0
Adenocarcinoma	2	0	2	0	0
HCC / ICC	0	28[c,e]	0	2[d]	0
Hemangiocarcinoma	0	0	2	0	0
Other causes of death[f]	29	10	17	9	4

[a] In the other two single-gene CKO mouse cohorts, MM was observed in 0 of 12 *Cdkn2a*$^{f/f}$ mice and 2 of 15 *Nf2*$^{f/f}$ mice, frequencies similar to a previous report (21).

[b] Abbreviations: HCC, hepatocellular carcinoma; ICC, intrahepatic cholangiocarcinoma; MM, malignant mesothelioma;

[c] 1 mouse had both MM and HCC, and 2 mice had MM as well as HCC and ICC;

[d] 1 mouse had both MM and ICC, and 1 mouse had MM and HCC;

[e] 14 of the 28 mice had both HCC and ICC;

[f] mostly aged mice, with moribund animals often found to have plaques, bladder obstructions, or lymphoproliferative lesions.